Appl. Phys. A (2015) 120:881–888
DOI 10.1007/s00339-015-9314-x

Applied Physics A
Materials Science & Processing

Synthesis of gold nanoparticle colloids by highly intense laser irradiation of aqueous solution by flow system

Muttaqin[1] · Takahiro Nakamura[1] · Shunichi Sato[1]

Received: 19 March 2015 / Accepted: 22 June 2015 / Published online: 2 July 2015

Abstract Highly intense femtosecond laser irradiation of a metallic ion solution is a potential technique to produce nanoparticles of noble metals and their alloys without any reducing agents. In addition, all-proportional solid-solution alloy nanoparticles of noble metals even with immiscible nature in a multimetallic system can be easily formed in the mixed ion solution. The method has many advantages compared to conventional chemical and/or physical methods with regard to not only the simplicity of the method itself but also the purity and the controllability of alloy composition of fabricated nanoparticles. However, the productivity of a stationary production system has been limited by the volume of a glass cuvette containing ion solution. In the present study, larger-scale production by applying a flow system of ion solution was demonstrated for improving the productivity. The influence of irradiation time and repetition rate of the femtosecond laser, and flow rate of the solution on the efficiency of nanoparticles formation was studied. The flow system showed similar results with the stationary system with respect to the mechanism for the nanoparticles formation. In addition, the pulse repetition rate was effective to increase the productivity by more than 200 % compared to the stationary system.

✉ Muttaqin
muttaqin@mail.tagen.tohoku.ac.jp

[1] Institute of Multidisciplinary Research for Advanced Materials, Tohoku University, Katahira 2-1-1, Aoba-ku, Sendai 980-8577, Japan

1 Introduction

Metal and alloy nanoparticles have attracted much attention because of their unique size-dependent optical, electrical and catalytic properties that have not been observed in the bulk form [1, 2]. Nanoparticles play a significant role in medical, bioscience and energy fields, because they are not only modified and functionalized but also combined with other materials inducing fascinating effects that are useful in many applications such as catalyst [3] and biosensor [4]. However, it is true that further improvement and control of size, purity, form, composition and stability are required for future applications [5].

Many chemical methods have been applied to expand the availability of nanoparticles with well-controlled size, feature and compositions for a wide variety of materials. Attempt for mass production was also promoted by a large-scale reaction system. However, the necessity of removing chemicals such as residual anion and reducing agent is an environmental issue for practical application [6–8]. In the last decade, different ways for metal nanoparticle fabrication have been demonstrated. Silver nanoparticles were fabricated in a continuous flow using a low-temperature microwave-assisted polyol process [9]. Monodispersed gold nanoparticles were successfully synthesized in ionic liquids using microfluidic platform [10]. Despite obtaining small particle size of 4.3 ± 0.5 nm in diameter, a series of additional procedures was necessary for purifying the synthesized nanoparticles. Pulsed laser ablation in liquids (PLAL) is another promising technique to obtain high-purity metal nanoparticles because of unnecessity of any reducing agents [11–14]. Mass production of pure metal nanoparticles was successfully performed by a flow system. The productivity was dramatically increased compared to stationary method [15]. However, it was not easy

to produce uniform alloy nanoparticles from a bulk target that is not solid-solution.

Highly intense femtosecond laser irradiation of metallic ion solution has been proposed as an alternative which does not require any reducing agents [16–18]. This technique is simple and one of the green routes for metal nanoparticle formation because it is a direct, one-step process for getting spherical-shaped pure metal nanoparticles with narrow size distribution. Even though laser pulses are used as energy sources for the synthesis of nanoparticles similar to PLAL, the phase of target material is completely different. Instead of using a solid target in the PLAL, metallic ion solutions are used as a target in the femtosecond laser irradiation method. By passing the laser beam through a focusing lens, an intense optical field is produced, which is energetic enough to break water or organic molecules into reactive components, i.e., solvated electrons, hydrogen radicals and hydroxyl radicals. Among them, solvated electrons and hydrogen radicals play an important role in the reduction in metal ions because of their high reduction potential. The detailed reaction mechanism of metallic ion reduction to produce metal nanoparticles is found elsewhere [18]. Not only pure metal but alloy nanoparticles in solid-solution form with high purity, narrow size distribution and fully tunable compositions have been successfully produced in both aqueous and organic solutions by the femtosecond laser irradiation [19–23]. However, the improvement in productivity of particles was required for practical application.

In this work, the improvement in productivity of nanoparticles by highly intense femtosecond laser irradiation is demonstrated by using a flow system of ion solution. All experiments were conducted at room temperature and atmospheric pressure. The influence of irradiation time and repetition rate of the femtosecond laser, and flow rate of the solution on the efficiency of nanoparticles production was studied in detail.

2 Experiment

As a precursor of gold nanoparticles formation, we used hydrogen tetrachloroauric(III) trihydrate powder ($HAuCl_4 \cdot 3H_2O$, >99.9 %), which was obtained from Wako Pure Chemical Industries, Ltd and used as received without any further purification. A gold solution was prepared by dissolving the salt in ultrapure water with the concentration of 2.5×10^{-4} M. The obtained solution was transparent and colorless. As shown in Fig. 1, 30 mL of the solution was placed in a reservoir and circulated by a peristaltic pump (MasterFlex® L/S easy load 3, Cole-Parker Instrument Co.) through a flow-type cuvette made of quartz glass. During the circulation at a fixed flow rate, femtosecond laser pulses with the pulse energy of 5–6 mJ were introduced perpendicular to the cuvette surface and focused by an aspheric lens [focal length: 8 mm, numerical aperture (NA): 0.5]. An UV–visible spectrometer (Ocean optics, HR 4000 CG-UV-NIR) was operated in situ to obtain the absorption spectra of the colloidal solution every 30 s during the irradiation. Table 1 shows laser specification and irradiation condition in the experiment. The stationary system, which was used in previous experiments without circulation of the solution, was also employed to compare the flow system. After a certain time of irradiation, UV–visible spectrum of the solution was also obtained using a UV–visible spectrometer (V-630 iRM, JASCO Co.) to evaluate the colloidal stability. A fraction of the solution (3 mL) dispensed in a rectangular quartz glass cuvette was used for spectrum measurement in the wavelength range of 200–800 nm. Moreover, TEM

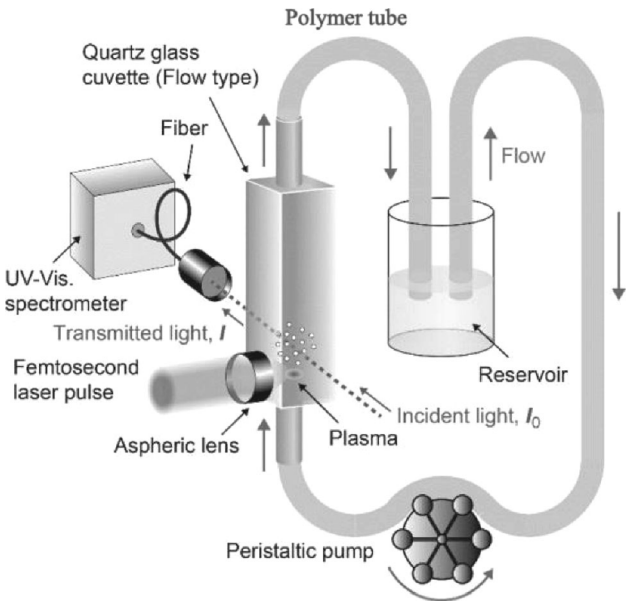

Fig. 1 Schematic of experimental setup

Table 1 Laser specification and irradiation condition

Femtosecond laser (Spitfire Pro, Spectra Physics Co. Ltd)	
Wavelength (nm)	800
Pulse width (fs)	100
Energy (mJ)	5–6
Beam diameter (mm)	10
Repetition rate (Hz)	100, 200, 300, 400
Focusing lens	Aspheric lens, *f*: 8 mm, NA: 0.5
Intensity (W/cm^2)	2.1×10^{14}
Flow rate (mL/s)	0.9, 1.7, 2.3, 3.3
Irradiation time (min)	15, 30, 60, 90, 120, 150

observation was conducted to analyze the morphological structure of fabricated gold nanoparticles using JEM2000EXII (JEOL Ltd.) at an acceleration voltage of 200 kV. TEM samples were prepared immediately after the laser irradiation by placing a few drops of the colloidal solution on a copper grid coated by carbon (Microgrid B, Okenshoji Co., Ltd.) and dried in a vacuum chamber at room temperature. Zeta (ζ)-potential of the fabricated gold nanoparticles was measured by using a nanoparticle analyzer (SZ100, HORIBA Ltd.).

3 Results and discussion

3.1 Formation of gold nanoparticles using stationary and flow systems

When the focused laser beam with the estimated intensity of 2.1×10^{14} W/cm^2 at the focal point was introduced into the gold solution both in the stationary and flow systems, fine bubbles, which were confirmed as oxygen and hydrogen gasses [24], were also observed around the focal point. The formation of these bubbles clearly indicates the dissociation of water molecules, leading to the generation of reactive species like solvated electrons, hydrogen radicals and hydroxyl radicals [25]. After a certain time of irradiation, the solution was changed from transparent to red-purple originated from surface plasmon resonance (SPR) of the formed gold nanoparticles.

Figure 2 shows the UV–visible absorption spectra of the gold ion solution before and after 30 min after irradiation by focused femtosecond laser pulses with the repetition rate of 100 Hz in a stationary system. As seen in the figure, the absorbance peak at 284.5 nm, which is attributed to the tetrachloroauric(III) ion ($[AuCl_4]^-$), disappeared after the laser irradiation. Instead, a clear absorption peak appeared at the wavelength of 515.5 nm, which is specific to the SPR of gold nanoparticles. This spectral change clearly exhibits that the gold ions were reduced to form gold nanoparticles by the high-intensity laser irradiation of the solution.

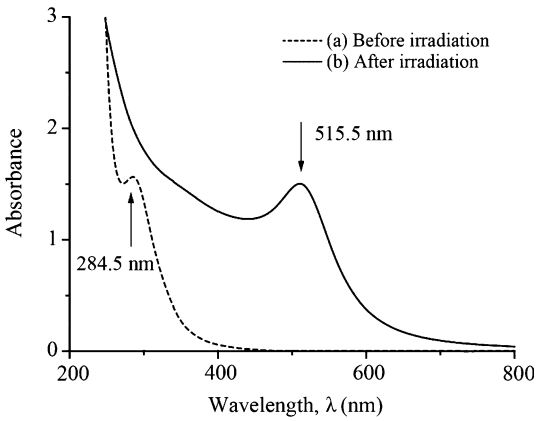

Fig. 2 UV–Vis absorption spectra of 2.5×10^{-4} M gold ion solution

During the laser irradiation, in situ observation of photoabsorption property of the gold ion solution was made by a UV–visible spectrometer to acquire instantaneous information regarding gold nanoparticles formation. Figure 3 displays absorption spectra of the gold ion solution every 30 s during the laser irradiation for (a) the stationary and (b) the flow system with the flow rate of 3.3 mL/s, while each inset depicts the variation of maximum absorbance (A_{max}) as a function of the irradiation time. From Fig. 3, we can see that the A_{max} of SPR increases and the peak position shifts to shorter wavelength with increasing the

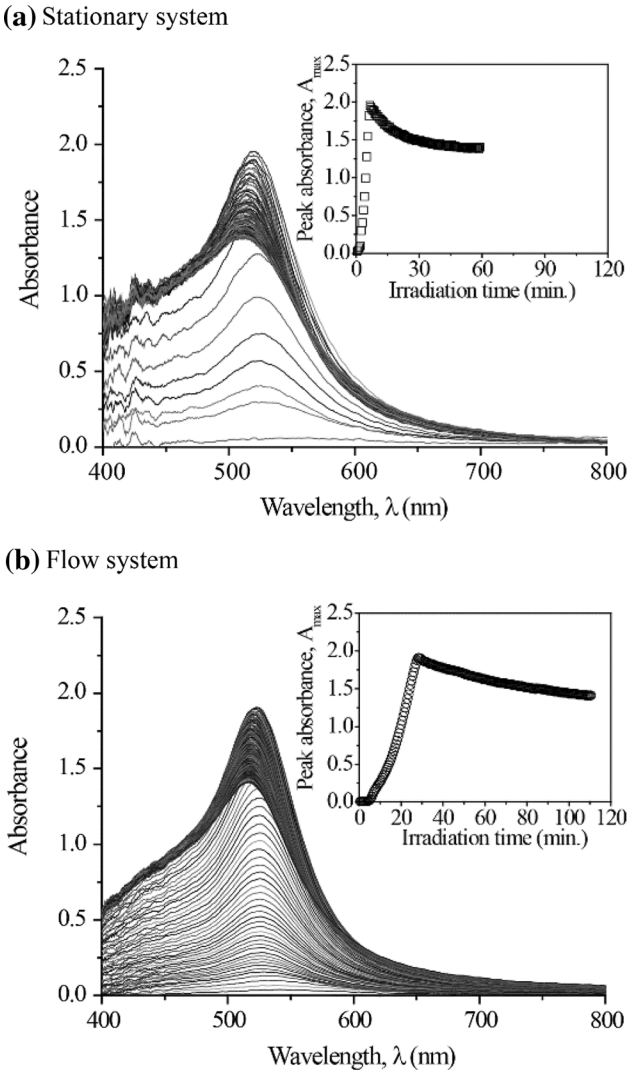

Fig. 3 *In situ* UV–visible absorption spectra of the gold ion solution during the laser irradiation for **a** the stationary system and **b** the flow system with the flow rate of 3.3 mL/s. The spectra were recorded every 30 s during the irradiation. Each *inset* shows the variation of the maximum absorbance (A_{max}) as a function of the irradiation time

irradiation time for both systems. The increase in the A_{max} indicates the gold nanoparticles formation, while the shift of the peak position means the decrease in particle size.

It is clearly seen in the insets that the A_{max} rapidly increases until reaching a maximum value and decreases gradually with the irradiation time for both systems. For the stationary system, similar observation has been reported, discussing that the particle formation consisted of nucleation, ripening and fragmentation processes [26]. The nucleation and ripening processes make progress until all the gold ions in the solution are reduced. These processes correspond to the period during which the A_{max} increases. After that, the fragmentation process, during which the A_{max} slowly decreases, takes place. It is suggested that these processes also took place for the flow system because of the quite similar behavior of the A_{max} as shown in the inset in Fig. 3b. Note that the difference of the timescale between the stationary and flow systems is attributed to the sample volume used in the experiment. Accordingly, it is indicated that 7 and 28 min are needed to reduce all the gold ions of 3 mL in the stationary system and 30 mL in the flow system, respectively. It is simply estimated that 70 min irradiation is necessary to complete 30 mL solution for the stationary system, indicating that the flow system has more than two times larger productivity of gold nanoparticles compared to the stationary system. Effective circulating of the gold solution in the flow system during laser irradiation contributes to the larger productivity of gold NPs formation because highly intense laser beam hits fresh, new solution for every single pulse resulting in effective reduction in gold ions.

3.2 Effect of irradiation time

In order to investigate the reaction of gold nanoparticles formation during laser irradiation in the flow system in detail, we observed the particles by TEM for different irradiation times of 15, 30, 60, 90, 120 and 150 min. Note that 15 min is in the way of growth process of A_{max}, 30 min is close to the time when A_{max}, and the longer irradiation times are in the decay process of A_{max}. A few drops of the gold solution were sampled for TEM observation. Figure 4 shows the TEM images and corresponding size distributions of the fabricated gold nanoparticles after 15, 30, 60, 90, 120 and 150 min irradiation. The size distribution profiles are obtained by direct observation of the fabricated nanoparticles from TEM micrographs.

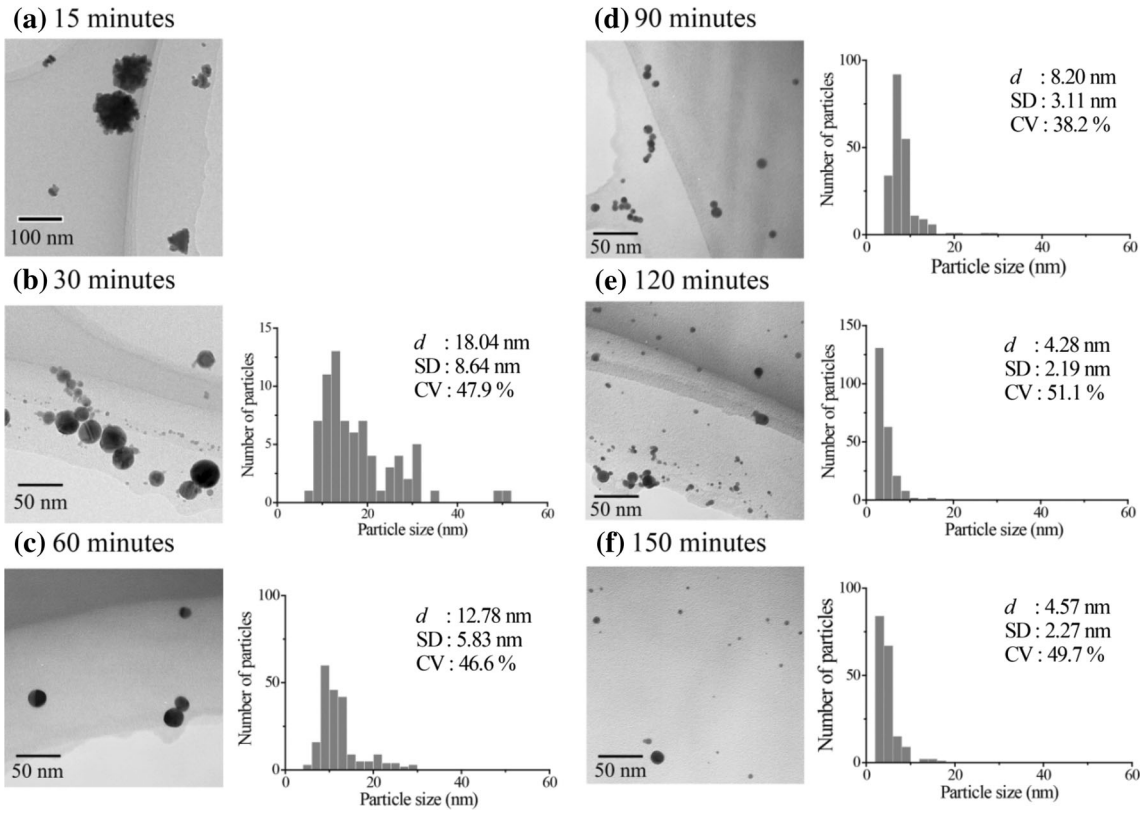

Fig. 4 TEM images and corresponding size distribution of gold nanoparticles with different irradiation times of **a** 15, **b** 30, **c** 60, **d** 90, **e** 120 and **f** 150 min. *d* is the mean particle diameter. SD and CV are the standard deviation and the coefficient of variation of particle size distribution, respectively

Gold nanoparticles fabricated at an irradiation time of 15 min were inhomogeneous, and the mean size was about 100 nm. In this case, it is difficult to draw size distribution because of the small number of fabricated particles on a TEM microgrid. According to the TEM micrograph, these large particles seem to consist of smaller particles forming aggregates. Then the fabricated particles became spherical with relatively broad size distribution at the irradiation time of 30 min at which the reduction in gold ions finished. After that, the fabricated particles became smaller, uniform in size and spherical as the irradiation time increased due to the fragmentation of the fabricated gold particles by succeeding high-intensity laser irradiation. The mean particle size of the gold nanoparticles as a function of the irradiation time is summarized in Fig. 5. It can be clearly seen that the mean particle size and the standard deviation expressed by error bar of the gold nanoparticles decrease with the irradiation time and then reach a plateau.

It is shown that longer laser irradiation more than 120 min was not effective for decreasing the average size. As can be seen in Fig. 5, the average size of the gold nanoparticles by 150 min irradiation was 4.57 nm, which is almost the same with that by 120 min irradiation. Accordingly, we conclude that 120 min irradiation is an optimum irradiation time to produce fine gold nanoparticles in the flow system, and the following experiments were performed by 120 min irradiation. This trend is the same as that in the stationary system in the preceding study [26]. Namely, the gold nanoparticles were formed through nucleation, ripening and fragmentation processes in the flow system.

3.3 Effect of flow rate of the solution

The productivity improvement in gold nanoparticles by femtosecond laser irradiation of aqueous solution was successfully demonstrated using the flow system in comparison with the stationary system. As a next step, the effect of flow rate of the solution on the efficiency of gold nanoparticles was investigated using the flow system for 120 min irradiation. Figure 6 shows the time variation of the maximum absorption (A_{max}) of the SPR peak in in situ UV–visible absorption spectra of the solutions with different flow rates of 0.9, 1.7, 2.3 and 3.3 mL/s.

It is clear that the required time for A_{max} being maximum showed no significant difference whichever flow rate was applied. TEM pictures of the fabricated particles and corresponding size distributions for different flow rates are shown in Fig. 7. There is no clear difference in average size and size distribution of the fabricated particles for different flow rates. This indicates that the flow rate has no appreciable effect on the resultant gold nanoparticles in the flow system. It has been reported that the fabricated gold nanoparticles that experienced the fragmentation process by high-intensity laser irradiation of solution in the stationary system have excellent colloidal stability without addition of any dispersants [27]. It was concluded that the colloidal stability is originated from negative charging of the gold nanoparticles due to partial oxidation through the fragmentation of gold particles in aqueous solution.

In this regard, the stability of the gold colloidal solution by the flow system was also investigated by means of time variation of UV–visible absorption spectra just after the laser irradiation until almost 1 month later as shown in Fig. 8.

As one can see in Fig. 8a, a series of UV–visible absorbance spectra of the gold colloidal solutions by the stationary system showed no change. This tendency was observed for the flow system. For different flow rates, the absorption spectra were almost same even after 26 days later, indicating that the colloidal solution was stable. As

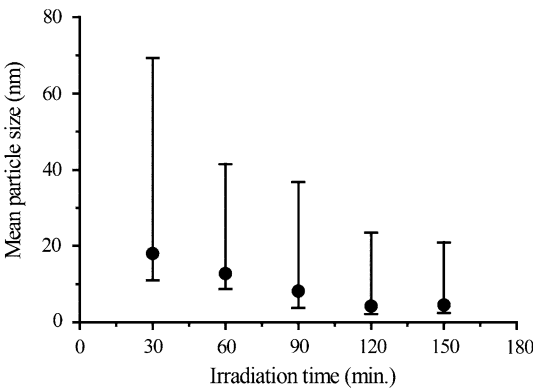

Fig. 5 Correlation between mean particle diameter of the gold nanoparticles as a function of the irradiation time

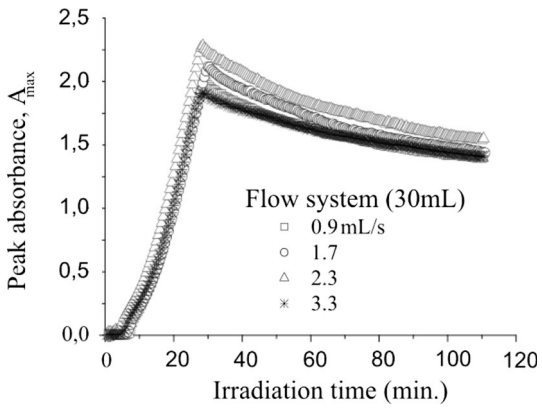

Fig. 6 Variations of the maximum absorbance (A_{max}) as a function of the irradiation time use a flow system with different flow rate conditions

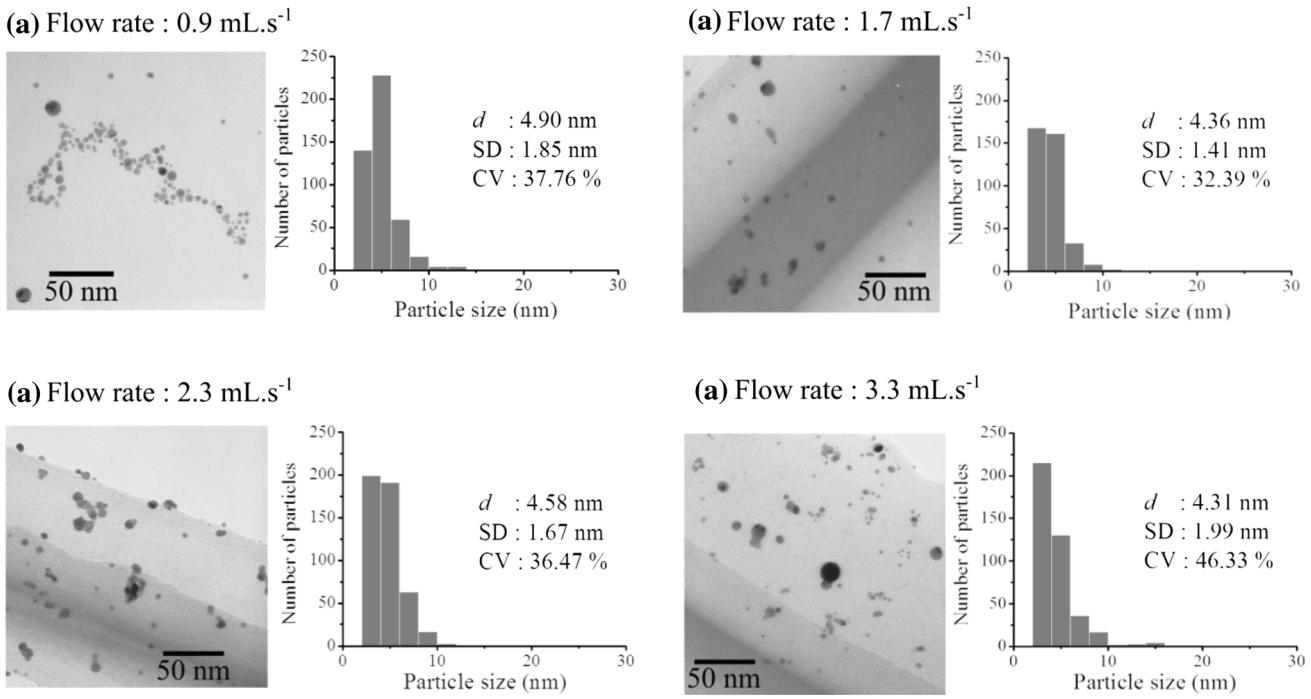

Fig. 7 TEM images and the corresponding size distribution of the gold nanoparticles fabricated in the flow system with different flow rates of **a** 0.9, **b** 1.7, **c** 2.3 and **d** 3.3 mL/s of 30 mL solutions, respectively

seen in Fig. 8c, d, the SPR peaks after 26 days were larger and slightly shifted to the longer wavelength side indicating minor degree of aggregation of gold nanoparticles. However, the colloidal solutions were stable because no any precipitation was observed. In ζ-potential measurement, the fabricated gold nanoparticles were negatively charged in all systems as presented in Table 2. These negative values were larger than that reported in the previous work (−30 mV) by Muto et al. [28], and they mentioned that the stability of the gold nanoparticles in solution is due to negative charge of the surfactant-free particles.

3.4 Effect of repetition rate of the pulses

It is reasonable to expect that the productivity of gold nanoparticles will be increased by applying higher repetition rate in the flow system. However, obtained result was contradictory to the expectation for the present system. Figure 9 shows the time variation of A_{max} in *in situ* UV–visible absorbance spectra of the gold colloidal solution by the flow system for different repetition rates of the laser pulses. In this experiment, the solution was irradiated for 120 min at the flow rate of 3.3 mL/s, which is the optimal experimental condition to achieve high productivity of gold nanoparticles in the flow system. At the repetition rate of 200 Hz, the A_{max} reached maximum at around 13 min, which was almost half compared to 28 min at 100 Hz, indicating that the productivity of gold particles was increased double as expected.

However, further increase in repetition rate did not give significant contribution to the time variation of A_{max}. As a result, higher repetition rate over 200 Hz was not effective to improve the productivity of gold nanoparticles in the present system. This unexpected result is attributed to the bubble formation around the focus by high-intensity laser irradiation of solution [29]. As stated in the preceding section, fine bubbles of oxygen and hydrogen gasses were generated around the focus as a consequence of photodecomposition of water molecules in the highly intense optical field. Most of bubbles were swept away from the focus by buoyancy and induced flow of solution at low repetition rate. However, the generated bubbles were not swept effectively when the repetition rate was increased over 200 Hz. Therefore, the excess bubbles acted as scatterer for introduced laser and then reaction efficiency is reduced. Accordingly, the productivity of gold nanoparticles will be improved at the repetition rate over 200 Hz by

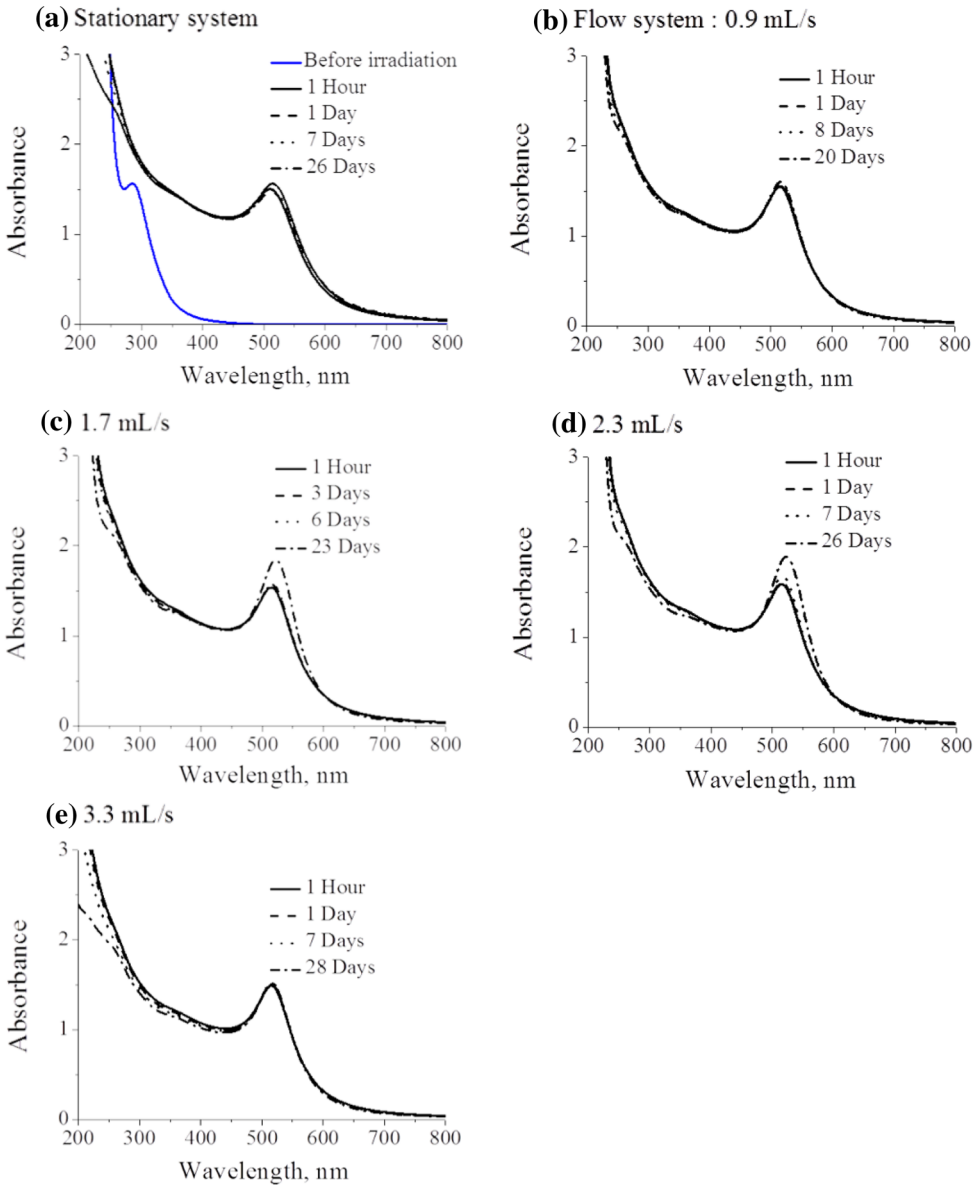

Fig. 8 Time variation of UV–Vis absorption spectra of the gold colloidal solution prepared by (**a**). The stationary system and the flow system with the flow rate of **b** 0.9, **c** 1.7, **d** 2.3 and **e** 3.3 mL/s

Table 2 ζ-potential measurements in different flow rates

Flow rate (mL/s)	ζ-potential (mV)
0.0	−57.1
0.9	−64.8
1.7	−55.7
2.3	−64.8
3.3	−65.5

applying the higher flow rate over 3.3 mL/s, which was the maximum rate of the peristaltic pump used in the experiment, to sweep out the generated bubbles from the focus effectively in the present flow system.

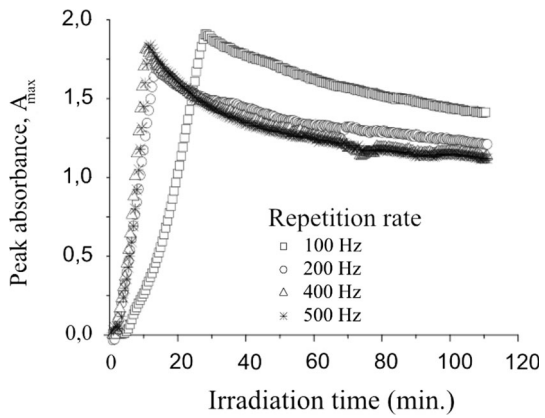

Fig. 9 Time variation of peak absorbance uses real-time UV–Vis absorbance spectra of the solution by the flow system with different repetition rates of the introduced laser pulse

4 Conclusion

Highly intense femtosecond laser irradiation of an ion solution is one of the promising tools for the synthesis of ultrapure metal/alloy nanoparticles. In this work, we succeeded in improving the productivity of gold nanoparticles using a flow system. The feature and property of gold nanoparticles prepared by the flow system with 30 mL solution were almost similar to that by the stationary system with 3 mL solution. In the stationary system, the productivity of gold nanoparticles in our study was 0.385 μg/s, which is similar to the previous work [30]. On the other hand, using the flow system, the productivity was improved more than 200 % compared to that in the stationary system, and that was 0.887 μg/s at 100 Hz and 1.785 μg/s at 200 Hz repetition rate. Although the productivity of the gold nanoparticles became double by increasing the repetition rate of the laser from 100 to 200 Hz, further increase in the repetition rate did not give higher productivity due to excess bubble formation around the focus which acted as scatterer for the incident laser pulses, resulting in the attenuation of the pulse energy at the focus. There is a possibility of further improving the productivity of metal nanoparticles by optimizing flow rate of the solution and the repetition rate of the introduced laser pulses in the flow system.

References

1. E. Roduner, Chem. Soc. Rev. **35**, 583 (2006)
2. S. Link, M.A. El-Sayed, Annu. Rev. Phys. Chem. **54**, 331 (2003)
3. A. Takami, H. Yamada, K. Nakano, S. Koda, Jpn. J. Appl. Phys. **35**, L781 (1996)
4. E. Katz, I. Willner, Angew. Chem. Int. Ed. **43**, 6042 (2004)
5. S. Barcikowski, G. Compagnini, Phys. Chem. Chem. Phys. **15**, 3022 (2013)
6. J. Nedderson, G. Chumanov, T.M. Cotton, Appl. Spectrosc. **47**, 1959 (1993)
7. M.S. Sibbald, G. Chumanov, T.M. Cotton, J. Phys. Chem. **100**, 4672 (1996)
8. M. Prochazka, P. Mojzes, J. Stepanek, B. Vlckova, P.Y. Turpin, Anal. Chem. **69**, 5103 (1997)
9. G. Dziko, A.B. Jarzębski, J. Nanopart. Res. **13**, 2533 (2011)
10. L.L. Lazarus, A.S.-J. Yang, S. Chu, R.L. Brutchey, N. Malmstadt, Lab Chip **10**, 3377 (2010)
11. F. Mafunè, J. Kohno, Y. Takeda, T. Kondow, J. Phys. Chem. B **104**, 9111 (2000)
12. A.V. Simakin, V.V. Voronov, G.A. Shafeev, R. Brayner, F.B.- Verduraz, Chem. Phys. Lett. **348**, 182 (2001)
13. A.V. Kabashin, M. Meunier, J. Appl. Phys. **94**, 7941 (2003)
14. B. Liu, Z. Hu, Y. Che, Y. Cheng, X. Pan, Appl. Phys. Lett. **90**, 044103 (2007)
15. S. Barcikowski, A. Menéndez-Manjón, B. Chichkov, M. Brikas, G. Račiukaitis, Appl. Phys. Lett. **91**, 083113 (2007)
16. T. Nakamura, Y. Mochidzuki, S. Sato, J. Mater. Res. **23**, 968 (2007)
17. T. Nakamura, H. Magara, Y. Herbani, S. Sato, Appl. Phys. A **104**, 1021 (2011)
18. Y. Herbani, T. Nakamura, S. Sato, J. Colloid Interface Sci. **375**, 78 (2012)
19. T. Nakamura, K. Takasaki, A. Ito, S. Sato, Appl. Surf. Sci. **255**, 9630 (2009)
20. Y. Herbani, T. Nakamura, S. Sato, J. Phys. Chem. C **115**, 21592 (2011)
21. T. Nakamura, Y. Herbani, S. Sato, J. Nanopart. Res. **14**, 785 (2012)
22. M.S.I. Sarker, T. Nakamura, Y. Herbani, S. Sato, Appl. Phys. A **110**, 145 (2013)
23. J.L.H. Chau, C.Y. Chen, M.C. Yang, K.L. Lin, S. Sato, T. Nakamura, C.C. Yang, C.W. Cheng, Mater. Lett. **65**, 804 (2011)
24. S.L. Chin, S. Lagacé, Appl. Opt. **35**, 907 (1996)
25. S. Pommeret, F. Gobert, M. Mostafavi, I. Lampre, J.-C. Mialocq, J. Phys. Chem. A **105**, 11400 (2001)
26. T. Nakamura, Y. Herbani, D. Ursescu, R. Banici, R.V. Dabu, S. Sato, AIP Adv. **3**, 082101 (2013)
27. J.P. Sylvestre, S. Poulin, A.V. Kabashin, E. Sacher, M. Meunier, J.H.T. Luong, J. Phys. Chem. B **108**, 16864 (2004)
28. H. Muto, K. Yamada, K. Miyajima, F. Mafune, J. Phys. Chem. C **111**, 17221 (2007)
29. A. Hahn, S. Barcikowski, B.N. Chichkov, J. Laser Micro Nanoeng. **3**, 73 (2008)
30. S. Petersen, S. Barcikowski, Adv. Funct. Mater. **19**, 1167 (2009)